Published in final edited form as:
J Eukaryot Microbiol. 2013 ; 60(2): 166–178. doi:10.1111/jeu.12019.

The Multilayered Interlaced Network (MIN) in the sporoplasm of the Microsporidium *Anncaliia algerae* is derived from Golgi

Peter M. Takvorian[a,b], **Karolyn F. Buttle**[c,*], **David Mankus**[c], **Carmen A. Mannella**[c], **Louis M. Weiss**[b,d], and **Ann Cali**[a]

[a]Department of Biological Sciences, Rutgers University, Newark, New Jersey, 07102

[b]Department of Pathology, Division of Tropical Medicine and Parasitology, Albert Einstein College of Medicine, 1300 Morris Park Avenue, Bronx, New York, 10461

[c]New York State Dept of Health, Resource for Visualization of Biological Complexity, Wadsworth Center, Empire State Plaza, Albany, New York, 12201-0509

[d]Department of Medicine, Division of Infectious Diseases, Albert Einstein College of Medicine, 1300 Morris Park Avenue, Bronx, New York, 10461

Abstract

This study provides evidence for the Golgi-like activity of the multilayered interlaced network (MIN) and new ultrastructural observations of the MIN in the sporoplasm of *Anncaliia algerae*, a microsporidium that infects both insects and humans. The MIN is attached to the end of the polar tubule upon extrusion from the germinating spore. It surrounds the sporoplasm, immediately below its plasma membrane, and most likely maintains the integrity of the sporoplasm, as it is pulled through the everting polar tube. Furthermore, the MIN appears to deposit its dense contents on the surface of the sporoplasm within minutes of spore discharge thickening the plasma membrane. This thickening is characteristic of the developmental stages of the genus *Anncaliia*. The current study utilizes transmission electron microscopy (TEM), enzyme histochemistry, and high voltage TEM (HVEM) with 3D tomographic reconstruction to both visualize the structure of the MIN and demonstrate that the MIN is a Golgi-related structure. The presence of developmentally regulated Golgi in the Microsporidia has been previously documented. The current study extends our understanding of the microsporidial Golgi and is consistent with the MIN being involved in the extracellular secretion in *Anncaliia algerae*. This report further illustrates the unique morphology of the MIN as illustrated by HVEM using 3D tomography.

Keywords

computerized tomography; electron microscopy; enzyme histochemistry; high voltage TEM; surface rendering; three-dimensional models

THE Microsporidia are a phylum of intracellular obligate eukaryotes closely related to the Fungi. While this group is extremely diverse, containing approximately 175 genera (Cali and Takvorian 2012) they all share several characteristics related to the spread of infection, including a highly resistant spore that is diagnostic for these organisms. The spore contains a

Correspondence P. Takvorian, Department of Biological Sciences, 195 university Avenue, Rutgers University, Newark, New Jersey 07102, USA Telephone number: 973 353 5364; FAX number: 973-353-5518 petetak@andromeda.rutgers.edu.

*This study is dedicated to the memory of Karolyn Buttle, an inspiring colleague and friend.

SUPPORTING INFORMATION Additional Supporting Information may be found in the online version of this article:

single coiled polar tube and sporoplasm, which provide for a unique means of infection by inoculation (Cali and Takvorian 1999; Vavra 1976). When the spores are in the proper environment to be activated, they germinate, resulting in the rapid and explosive eversion of the polar tube (this structure is often called the polar filament when it is inside the spore as it contains electron-dense material prior to germination). The polar tube exits the anterior end of the spore and it may then penetrate a host cell or perhaps invaginate the host cell plasma membrane creating a unique microenvironment in which penetration of the host cell occurs. During the polar tube eversion process, the sporoplasm is transferred from the spore, through the extruded polar tube into the new host cell (Cali et al. 2002; Takvorian et al. 2005). Sporoplasms successfully transferred into a host cell develop in the intracellular environment completing the life cycle of this parasite and thereby establishing new infections. Usually sporoplasms and meronts (proliferative stages of development) are surrounded by a traditional plasma membrane that “thickens” (by secretions) only at the onset of sporogony. An exception to this general trend is found in *Anncaliia* (*Brachiola, Nosema*) *algerae* (Franzen et al. 2006; Lowman et al. 2000; Vavra and Undeen 1970), which forms a thickened plasma membrane from sporoplasm (within 1-h post inoculation) through all developmental stages (Avery and Anthony 1983).

While much attention has been given to the various intracellular developmental cycles of microsporidia, their spores, and the myriad of variations in structure and host parasite interaction, relatively little attention has been paid to the sporoplasm, which is a common feature to them all, but difficult to observe (Cali et al. 2002; Scarborough-Bull and Weidner 1985; Vavra and Larsson 1999; Weidner et al. 1999). Some reasons for this include the fact that of the 1,200 plus species, only a few have spores that can be activated in vitro using germination solution and most of these solutions only activate a small percentage of spores. In addition, sporoplasms are difficult to identify/differentiate in the host cytoplasm, and due to their small size and numbers compared to the size of a host cell and the number of noninfected cells the difficulty of finding them in thin sections, is great.

In vitro studies of spore germination and the sporoplasm by our laboratory group have improved our understanding of the interactions of various spore structures involved in the transfer of the sporoplasm from the spore through the polar tube. These studies resulted in the description and naming of an organelle, the multilayered interlaced network (MIN), identified in both the spore and the sporoplasm (Cali and Takvorian 2001; Cali et al. 2002) and clarified other structures and events related to this process (Takvorian et al. 2005). The present study provides a fundamental characterization of the MIN, a microsporidial organelle. It apparently has at least two functions. The first is structural; positioned immediately below the plasma membrane, it surrounds the sporoplasm, serving as the attachment site to the polar tube, while maintaining sporoplasm integrity as it travels through the polar tube during eversion from the spore. The second function appears to be secretory, transferring its contents to the sporoplasm cell surface within minutes of being deposited into the host cell cytoplasm. These secretions form the sporoplasm’s “thickened plasmalemma” and the MINs’ remnants form cytoplasmic vesicles (Cali and Takvorian 2001; Cali et al. 2002; Takvorian et al. 2005) and we hypothesized that the MIN could be a unique adaptation of the *A. algerae* Golgi. Golgi-related activity in Microsporidia was first demonstrated with enzyme histochemistry in *Glugea stephani* sporoblasts during polar tube formation (Takvorian and Cali 1994, 1996). Subsequently, Beznoussenko et al. (2007) identified Golgi in all developmental stages of *Paranosema*, with the exception of sporoplasms. The current study has enabled the visualization of the 3D structure of the MIN (Cali et al. 2002) and demonstration of its Golgi-like activity in the sporoplasm of the microsporidium, *Anncaliia algerae*.

MATERIALS AND METHODS

Spore propagation

Anncaliia algerae spores were propagated in rabbit kidney cells (RK-13; ATCC CCL-37) and collected from culture media and stored in sterile distilled water at 4 °C as previously described (Cali et al. 2002).

Germination of spores

One ml aliquots of *A. algerae* spores (4×10^7 ml) were placed in several 1.5-ml microfuge tubes, and 0.5-ml of germination solution containing 0.003 M potassium chloride, 0.175 M sodium chloride, and 0.001 M calcium chloride dissolved in a 0.02 M tris-base (hydroxmethyl aminomethane) buffer pH 8.5 (all purchased from Sigma Chemical Co., St. Louis, MO) was added to each tube and allowed to react for 1–5 min. The tubes were then centrifuged at 5,000 × *g* for 30-s to obtain a pellet of intact and discharged spores, discharged polar tubes, and sporoplasms as previously described (Cali and Takvorian 2001).

Transmission electron microscopy of germinated sporoplasms

After removal of the supernatant (germination buffer and water), the pellets containing *A. algerae* spores and sporoplasms in each individual tube were then fixed in 0.1 M (w/v) cacodylate-buffered 2.5% (v/v) glutaraldehyde for 30 min at room temperature, the fixative removed and fresh 4 °C fixative added for 2–4 h. Controls had distilled water substituted for germination buffer. All samples were then postfixed in 0.1 M cacodylate-buffered 1% (w/v) OsO_4 for several hours, dehydrated in graded ethanols, propylene oxide, and infiltrated with Epon resin. The pellets were then transferred to BEEM® capsules filled with resin and hardened into blocks. Thin sections were cut, stained with 1% aqueous uranyl acetate and lead citrate, and examined with an FEI (Hillsboro, OR) Tecnai 12 transmission electron microscope (TEM) at the Rutgers Newark electron microscopy facility. Ten independent sporoplasms were identified and examined for these studies.

Transmission electron microscopy of enzyme histochemically (EH) labeled Golgi and ER in infected cell cultures

RK-13 cells were plated and grown on several 4 chamber Nunc® (Nalge Nunc Internat., Rochester, NY) culture slides for 24-h. The cell culture medium was removed and 200-μl of inoculum, containing 4.5×10^7 *A. algerae* spores/ml in fresh media was added to each chamber and allowed to incubate for 1-h at 32 °C. The inoculum was removed and the cultures were preserved in fixative containing 2% (w/v) paraformaldehyde, 0.5% (v/v) glutaraldehyde, in 0.15 M (w/v) cacodylate buffer with 4% (w/v) sucrose for 20 m. The chambers were rinsed several times with cacodylate buffer and stored in buffer at 4 °C.

To demonstrate the presence of *trans*-Golgi cisternae, a thiamine pyrophosphatase (TPPase) reaction was used as previously reported (Takvorian and Cali 1994). Briefly, a tris-maleate buffer pH 7.2, containing NaOH, $MnCl_2$, lead nitrate, and sodium-thiamine pyrophosphate (STP) substrate was used as the reaction medium. Control solutions were incomplete (sucrose substituted for STP), or the complete reaction medium was inhibited by the addition of 0.05 M NaF.

To demonstrate the presence of *cis*-Golgi cisternae and segments of the ER, a nucleoside diphosphatase (IDPase) reaction was used as previously reported (Takvorian and Cali 1996). Briefly, a tris-maleate buffer pH 7.2, containing NaOH, $MnCl_2$, lead nitrate, and inosine-5′-diphosphate (IDP) substrate was used as the reaction medium. Control solutions were incomplete (sucrose substituted for IDP), or the complete reaction medium was inhibited by the addition of 0.05 M levamisol (Sigma-Aldrich, St. Louis, MO). The storage buffer was

removed from the chambers and 200 μl of TPPase reaction media or IDPase reaction media were added to the appropriate chambers. Control solutions were added to the remaining chambers. The chamber slides were covered and then incubated for 1 h at 29 °C. After incubation, each chamber was emptied of reaction media and rinsed several times with fresh cacodylate buffer. The cells in each chamber were then fixed in 0.1 M cacodylate-buffered 2.5% glutaraldehyde for 30 min at room temperature; these samples were not postfixed with OsO_4. The cells were then dehydrated in graded ethanols, propylene oxide, and infiltrated with Epon resin. Resin filled BEEM® capsules were inverted over the cells and hardened at 60 °C. After hardening, the slides were placed in a shallow layer of liquid nitrogen and the capsules containing the cells were removed from the slides. The blocks were trimmed and thin sections were cut, collected on copper grids, stained with only 1% aqueous uranyl acetate, and examined with the FEI Tecnai 12 TEM operated at 80 kV at the Rutgers Newark electron microscopy facility. From 5 to 10 sporoplasms were identified and examined for each enzyme histochemical stain used.

High voltage electron microscopy (HVEM) and tomography

The blocks of propagated, germinated, *Anncaliia algerae* spores prepared for thin section TEM (Cali et al. 2002) were also used for 3D analysis using HVEM. Several 400-nm-thick sections were cut from the Epon blocks of activated *A. algerae* spores, placed on copper grids, stained with uranyl acetate, lead citrate, and then colloidal gold particles (10 nm diam.) were applied to one side as alignment markers. Tilt series were recorded on an AEI EM7 HVEM operated at an accelerating voltage of 1,000 kV. The images were recorded around two orthogonal tilt axes, each over an angular range of ± 60° at tilt intervals of 2°. These images were digitized (4 nm/pixel) and aligned as previously described (Penczek et al. 1995). Tomographic reconstructions were computed using the images that successfully aligned (typically 100 or more) using the weighted back-projection method (Radermacher 1992), implemented in the SPIDER image processing system (Frank et al. 1996). Nominal resolution for a 400-nm-thick section was 12-nm in the plane of the section and 18-nm normal to the plane (Radermacher 1992). Three-dimensional models of membrane surfaces were generated by isodensity surface rendering following denoising using anisotropic diffusion (Frangakis and Hegerl 2001). Visualization was carried out using IRIS Explorer® (NAG, Downers Grove, IL) and Amira® (Visage Imaging Inc., San Diego, CA). The HVEM imaging and tomographic reconstructions were performed at the Resource for Visualization of Biological Complexity, Wadsworth Center, New York.

RESULTS

Morphology of the MIN and its polar tube association

TEM of extruded sporoplasms, fixed within 3–5 min post application of germination medium revealed the presence of numerous activated spores, extruded polar tubes, empty spores, and spherical to ovoid cells, some with the polar tube still attached. These cells, identified as sporoplasms, contain diplokaryotic nuclei surrounded by a relatively granular homogeneous cytoplasm and an elaborate interconnected tubular-vesicular network. This network is located immediately under the sporoplasm plasma membrane, surrounds the sporoplasm, and has been described as a multilayered interlaced network (MIN) (Fig. 1–3). The MIN is variable in appearance but the spacing within the interconnecting network is consistent, averaging 44–55 nm (Fig. 2, 3). The thickness of the MIN layer varies around the sporoplasm, ranging from a single layer of approximately 60-nm to over 1,000-nm (Fig. 3). The network appears to be tubular and contains electron-dense material when routinely processed for standard TEM (Fig. 1–6) The MIN is connected directly to the sporoplasm cell plasma membrane by many cross connections (Fig 4–6) as previously published (Cali et al. 2002; Fig. 20, 21).

Some of the extruded polar tubes were attached to the empty spore shells and other polar tubes remained attached to their sporoplasm for several minutes post extrusion (Fig. 4). The continuity of the MIN with the polar tube was observed in several sections, which contained both. Longitudinal (Fig. 5) or cross-section cuts (Fig. 6) of the polar tube clearly illustrate the multiple attachment sites (seven in one section) between the MIN and the polar tube in one plane of section. These traditional thin section TEM images of sporoplasms illustrate both the location and structure of the MIN. The images of the polar tube interconnected with the MIN demonstrate the site of attachment in the sporoplasm.

Enzyme histochemical evidence of the relationship of MIN to Golgi

Inosine-diphosphatase (IDPase) activity is a well-documented histochemical indicator of the *cis*-Golgi and in some cells the endoplasmic reticulum (ER), when inosine-5-diphosphate (IDP) is used as the substrate. Demonstration of *cis*-Golgi activity is provided by deposition of electron-dense reaction product (RP) on the appropriate cisternae. The presence of IDPase RP in the Golgi of the host, rabbit kidney cells, serves as a positive control (Fig. 7, 8). Discharged sporoplasms located exterior to the host cells (Fig. 9) or in their cytoplasm (Fig. 10, 11) contained positive RP that was limited to the MIN. This histochemical procedure indicates the presence of *cis*-Golgi and in some cells, the ER; thus a second technique specific for only Golgi was utilized.

The enzyme thiamine pyrophosphatase (TPPase) is found in the *trans*-Golgi cisternae and exclusively reacts with its substrate, sodium-thiamine pyrophosphate, depositing RP in only the *trans*-cisternae of the Golgi and thus, is an excellent Golgi marker. The presence of fine particulate RP exclusively in the rabbit host cells' Golgi and not in its ER, is indicative of "classic *trans*-Golgi" labeling and also serves as a positive control (Fig. 12) demonstrating the specific labeling properties of this reaction (additional negative controls are provided for both of the Golgi stains in Fig. S1). Sporoplasms extruded in cell culture contained TPPase RP in the tubules of the MIN, thus indicating a positive reaction specifically for Golgi (Fig. 13–16). A sporoplasm in the process of being phagocytized by the host cell also demonstrates several areas of RP at its periphery (Fig. 17). The ultrastructural enzyme histochemical labeling of the host cell *cis/trans*-Golgi cisternae and the presence of both TPPase and IDPase RP in the MIN of the sporoplasm, illustrate the presence of both *cis* and *trans*-Golgi enzymes in the MIN.

High voltage electron microscopy (HVEM) and 3D reconstruction

Dual axis HVEM tomography was used to reconstruct the MIN concentrated at one end of the sporoplasm in a thick (400 nm) section. Figure 18 shows six 4-nm-thick slices taken from increasing depths in the reconstructed volume or tomogram. (A "walk-through" movie of all the slices in the volume is provided as Movie S1.) Membrane structures from 30 areas of the MIN were measured and found to range from 20 to 28-nm in thickness. The presence of the polar tube in relation to the sporoplasm as well as the MIN itself, are orienting features. While the density of the plasma membrane is faint in some regions on the sporoplasm perimeter, it is predominantly continuous through the volume, indicating that it encloses the entire cytoplasm including the MIN region. (The basic continuity of the plasma membrane and its close proximity to and local contacts with the membrane delimiting the MIN is demonstrated in Movie S2.)

Following denoising of the reconstructed volume, various 3D models of isodensity surfaces were generated at different scales. Figure 19 is a surface model of a large segment of the sporoplasm, measuring $2.9 \times 3.0 \times 0.3\ \mu m^3$.

While the MIN structure appears somewhat like a lace network in two dimension (Fig. 3, 4), the tubular nature of the structures become apparent when the reconstructed volume is rendered as isodensity surfaces, with a portion of the plasma membrane removed so one can discern the MIN structure. Rotational views of the 3D surface model of the MIN (Fig. 20) and the movie in Supporting Information (Movie S3) clearly illustrate the overall complexity of the tubular network and the many interconnections. For a better understanding of the local 3D structure within the MIN region, one subvolume ($266 \times 403 \times 300$ nm^3) was isolated and the surface rendering optimized according to the local density ranges. The side view (Fig. 21) shows the external surfaces of this subregion in pink, denser surfaces in dark blue, and the surrounding region of the MIN in light blue. Higher magnifications of the region viewed at different angles reveal different aspects of the MIN's 3D structure (Fig. 22, 23). The view in Fig. 22 clearly demonstrates the "sheet-like" nature of these fenestrated membranes, the flattened saccules and the many interconnections of the tubular portions of the structure. The convoluted twists and interconnections of these tubules are visible by rotating the model as in Fig. 23. This view demonstrates the dilations and constrictions of the tubules as they intersect with each other. The model in Fig. 24 (annotated with the dimensions along each axis) shows the numerous branched varicose tubules which anastomose in several areas.

The HVEM tomographic reconstruction indicates that the MIN is a complex of intersecting branched tubules that interconnect with large areas of flattened fenestrated sheets of membranes that narrow into constrictions, with tubular structures emanating from some of these constrictions. This structure is located immediately below the sporoplasm plasma membrane with many connections to it. During this study of the MIN structure, no coated or uncoated vesicles (COP-I, II) or buds (clathrin-like bodies) were observed by any of the imaging methods. Nor was a perinuclear "traditional" Golgi organization of stacked flattened ribbon-like cisternae present.

DISCUSSION

In the current study, TEM images of thin sections of *A. algerae* germinated sporoplasms reveal the presence of the elaborate network of the MIN immediately below the plasma membrane and with multiple attachments to the everted polar tubule. The thickness of the MIN varies from a single layer to multiple layers. The MIN is connected to the sporoplasm cell plasma membrane by many cross connections, probably providing the means of transport of its contents to the cell surface (Fig. 1, 4, 5, 6). The extruded end of the polar tubule is also attached to the MIN in multiple locations (Fig. 6). These observations are consistent with the original description of the MIN (Cali et al. 2002). The current study utilized multiple methodologies (e.g. TEM, enzyme histochemistry, and HVEM) to demonstrate that the MIN is a Golgi-related structure.

Golgi is a major part of the cell endomembrane system. Classic eukaryotic Golgi are composed of stacked lamellar cisternae, coated buds, and vesicles. Genomic studies demonstrate that Golgi-associated proteins are conserved in all eukaryotes (Mowbrey and Dacks 2009), suggesting that Golgi evolved in an early ancestral eukaryotic cell. Based on this common ancestry, one might expect that its structure would also be conserved; however, this is not the case in *Giardia*, *Cryptosporidia*, and Microsporidia (Mowbrey and Dacks 2009). In *Giardia* (Lujan et al. 1995) and *Cryptosporidia* (Tetley et al. 1998) the presence of a discernable Golgi structure is lacking. *Giardia* trophozoites undergo a developmental induction of Golgi enzyme activities, which correlates with differentiation into cysts (Lujan et al. 1995). In *Giardia*, the classic Golgi structure has been "*lost*" during reductive evolution and a modified organelle (encystation-specific vesicles) functions as a *trans*-Golgi during cyst wall formation (Konrad et al. 2010). The location of the Golgi-related vesicles in

encysting *Giardia lamblia*, have been demonstrated to be directly under the plasma membrane (Touz et al. 2004). Many parasitic organisms require an extracellular surface coat for protection and transmission into a new host cell. The presence of secretions on the *A. algerae* sporoplasm surface immediately after germination (Avery and Anthony 1983; Takvorian et al. 2005) may be necessary for transmission of this organism to its host cell.

In the microsporidium *Encephalitozoon cuniculi* genome sequence, a number of Golgi-associated protein sequences were identified (Katinka et al. 2001); however, EM did not demonstrate classic Golgi (Mowbrey and Dacks 2009). Microsporidian Golgi was originally reported to consist of a "meshwork of vesicles" referred to as "a primitive Golgi zone", as it did not resemble typical Golgi (Vavra 1965). It was subsequently appreciated that these Golgi may change in appearance depending on the life cycle stage of the organism, e.g. the Golgi of *Nosema apis* becomes a more prominent tubular network as the developmental cycle proceeds (Youssef and Hammond 1971). Golgi in the Microsporidia has been implicated in formation of the polar tube and invasion apparatus. For example, in *Glugea stephani* sporoblasts, the branching tubular structures associated with polar tube formation were histochemically labeled by thiamine pyrophosphatase (TPPase) (Takvorian and Cali 1994), which is specific for the *trans*-membranes of the Golgi apparatus (Farquhar et al. 1974; Iwamura et al. 2001; Novikoff and Novikoff 1977). In addition, in the developing polar tube inosine-diphosphatase (IDPase) a *cis*-Golgi and endoplasmic reticulum histochemical label (Novikoff 1976; Novikoff and Goldfischer 1961), was demonstrated in membranes involved in polar tube formation (Takvorian and Cali 1996). The presence of these two histochemical Golgi labels on the tubular structures and membranes associated with polar tube formation, clearly demonstrated the presence of Golgi with *cis* – *trans* properties in the microsporidial sporoblast. Further evidence for functional Golgi in the Microsporidia and the involvement of Golgi in the development of the polar tube and invasion apparatus is provided by the presence of posttranslational modifications of proteins making up the polar tube (Delbac et al. 1998, 2001; Keohane and Weiss 1999; Keohane et al. 1994, 1996). Xu et al. (2004) demonstrated O-glycosylation in *Encephalitozoon hellem* and *A. algerae* polar tubes. They suggested that O-mannosylated glycoproteins probably have a functional significance in the invasion process by affording protection from degradation during spore germination in the host intestinal tract and by creating a "sticky" polar tube surface for adhesion to host cells to aid penetration.

Beznoussenko et al. (2007) utilized Microsporidia of the genus *Paranosema* as a model of a minimal cell system for Golgi function and demonstrated a lack of transport vesicles (both COP-I and COP-II). Despite using a number of sophisticated methodologies to identify the presence of COP-I and COP-II vesicles usually associated with Golgi, they determined that microsporidian Golgi, although having histochemical properties of Golgi, do not form vesicles. Instead, they have branching or varicose tubules in a network connected to the ER and plasma membrane (Beznoussenko et al. 2007). Incorporating several methodologies, including immuno-microscopy, ultrastructural studies, and 3D reconstructions from thin sections, they were able to illustrate the presence of a Golgi apparatus in meronts, sporonts, sporoblasts, and spores. They concluded that the Golgi appears as a network of branching tubules that have classic Golgi histochemical features. The microsporidian sporoplasm was absent from their list of stages and a number of early reports suggest that freshly discharged sporoplasms do not have a Golgi (Ishihara 1968; Weidner 1972; Weidner and Trager 1973). However, the sporoplasm has been demonstrated to have an organelle, the MIN, which resembles the microsporidial Golgi in structure (Cali et al. 2002), but its biochemical function had not been previously demonstrated.

In the current study, sporoplasms (both in the host cell cytoplasm and free in the cell culture medium) were labeled for *cis* and *trans*-Golgi activity with IDP and TPP electron

cytochemistry, respectively. The rabbit kidney host cell cytoplasm provided the positive control demonstration of these labels in mammalian cell Golgi. Negative controls (full incubation medium minus substrate) of sporoplasms and host cells were devoid of reaction product (Fig. S1). The MIN of the sporoplasms in host cell cytoplasm as well as free in the medium were labeled with dense reaction product, demonstrating Golgi-related enzyme activity. The presence of the Golgi histochemical markers at the interface of host cell cytoplasm and the sporoplasm plasma membrane, suggest that the MIN can act as a secretory organelle providing the surface coat associated with the precocious thick plasma membrane characteristic of *A. algerae*.

High voltage electron microscopy of thick sections of cells and organelles coupled with computerized tomography has been used to study the organization of various cell components (McIntosh et al. 2005), including the Golgi in several mammalian cell types (Ladinsky et al. 1994, 1999, 2002; Nagata 2000; Rambourg et al. 1979). These studies indicate that the Golgi is organized as a ribbon and is composed of cisternae that are bridged and form networks. In the yeast, *Saccharomyces cerevisiae*, the Golgi is a tubular network of intersecting nodular dilations that vary in size and are interspersed throughout the cell (Rambourg et al. 2001). HVEM and computerized tomography have also been used to study mitochondria in *Cryptosporidium parvum* (Keithly et al. 2005) and the polaroplast membrane organization in the anterior portion of *A. algerae* microsporidial spores (Takvorian et al. 2006). The present study utilized 400-nm sections of the sporoplasm coupled with computerized tomography to provide 3D information about the organization of cellular constituents, such as membrane complexes at excellent resolution. The tomographic reconstruction demonstrated the sheet-like or membranous nature of the MIN and the many interconnections between the layers (features difficult to visualize with 2D TEM). Our 3D models of the MIN-Golgi are similar to the reconstructions of the microsporidian Golgi in *Paranosema*, in that they both demonstrate numerous interconnected tubules. Our studies also concur with Beznoussenko et al. (2007) in that COP-I and II vesicles are not present. In *A. algerae*, the MIN- Golgi remains connected to the cell plasma membrane (Fig. 18a, c; Movie S2) for secretion, which may eliminate the need for transport vesicles. The MIN does not appear connected to other organelles and it dissipates soon after spore germination.

Finally, the data presented in this study demonstrates that the MIN is unique in its location and has a very complex structure with characteristic Golgi-like activity and functions. This study has enabled us to extend the understanding of Golgi in Microsporidia and its presence from polar tube formation in sporogony (Beznoussenko et al. 2007; Takvorian and Cali 1994, 1996) at which time its products are for intracellular development, to its presence and activity in the germinating spore and sporoplasm, where the products are for extracellular secretion via the MIN-Golgi apparatus.

Supplementary Material

Refer to Web version on PubMed Central for supplementary material.

Acknowledgments

The authors (PMT and AC) acknowledge Cyrilla Pau for her many years of dedicated and outstanding assistance in our laboratory. This study was supported by NIH grant 5R01AI031788-19.

HVEM tomography at Wadsworth's Resource for Visualization of Biological Complexity (RVBC) was supported by the National Center for Research Resources, NIH, grant RR01219.

LITERATURE CITED

Avery SW, Anthony DW. Ultrastructural study of early development of *Nosema algerae* in *Anopheles albimanus*. J. Invertebr. Pathol. 1983; 42:87–95. [PubMed: 6411825]

Beznoussenko GV, Dolgikh VV, Seliverstova EV, Semenov PB, Tokarev YS, Trucco A, Micaroni M, Di Giandomenico D, Auinger P, Senderskiy IV, Skarlato SO, Snigirevskaya ES, Komissarchik YY, Pavelka M, De Matteis MA, Luini A, Sokolova YY, Mironov AA. Analogs of the Golgi complex in microsporidia: structure and avesicular mechanisms of function. J. Cell Sci. 2007; 120:1288–98. [PubMed: 17356068]

Cali A, Takvorian PM. *Brachiola algerae* Sporoplasms. J. Eukaryot. Microbiol. 2001; 48:81S–82S. [PubMed: 11906089]

Cali, A.; Takvorian, PM. Microsporidia. In: Margulis, L.; Chapman, MJ., editors. The Handbook of Protoctista. 2nd ed. Jones and Bartlett Learning; Burlington, MA: 2012. (in press)

Cali, A.; Takvorian, PM. Developmental morphology and life cycles of the microsporidia. In: Wittner, M.; Weiss, LM., editors. The Microsporidia and Microsporidiosis. ASM Press; Washington, DC: 1999. p. 85-128.

Cali A, Weiss LM, Takvorian PM. *Brachiola algerae* spore membrane systems, their activity during extrusion, and a new structural entity, the multilayered interlaced network, associated with the polar tube and the sporoplasm. J. Eukaryot. Microbiol. 2002; 49:164–174. [PubMed: 12043963]

Delbac F, Peuvel I, Metenier G, Peyretaillade E, Vivares CP. Microsporidian invasion apparatus: identification of a novel polar tube protein and evidence for clustering of ptp1 and ptp2 genes in three *Encephalitozoon species*. Infect. Immun. 2001; 69:1016–1024. [PubMed: 11159998]

Delbac F, Peyret P, Metenier G, David D, Danchin A, Vivares C. On proteins of the microsporidian invasive apparatus: complete sequence of a polar tube protein of *Encephalitozoon cuniculi*. Mol. Microbiol. 1998; 29:825–834. [PubMed: 9723921]

Farquhar MG, Bergeron JJM, Palade GE. Cytochemistry of Golgi fractions prepared from rat liver. J. Cell Biol. 1974; 60:8–25. [PubMed: 4358430]

Frangakis AS, Hegerl R. Noise reduction in electron tomographic reconstructions using nonlinear anisotropic difusion. J. Struct. Biol. 2001; 135:239–250. [PubMed: 11722164]

Frank J, Radermacher M, Penczek P, Zhu P, Li Y, Ladjadj M, Leith A. SPIDER and WEB: processing and visualization of images in 3D-electron microscopy and related fields. J. Struct. Biol. 1996; 116:190–199. [PubMed: 8742743]

Franzen C, Nassonova ES, Scholmerich J, Issi IV. Transfer of the members of the genus *Brachiola* (Microsporidia) to the genus *Anncaliia* based on ultrastructural and molecular data. J. Eukaryot. Microbiol. 2006; 53:26–35. [PubMed: 16441582]

Ishihara R. Some observations on the fine structure of sporoplasm discharged from spores of a microsporidian, *Nosema bombycis*. J. Invertebr. Pathol. 1968; 12:245–258.

Iwamura E, Nascimento S, Sesso A. In vitro cytochemical studies of the Golgi apparatus of pancreatic acinar cells exposed to drugs that inhibit the transport of membranes and proteins. J. Submicrosc. Cytol. Pathol. 2001; 33:83–92. [PubMed: 11686413]

Katinka MD, Duprat S, Cornillot E, Metenier G, Thomarat F, Prensier G, Barbe V, Peyretaillade E, Brottier P, Wincker P, Delbac F, El Alaoui H, Peyret P, Saurin W, Gouy M, Weissenbach J, Vivares CP. Genome sequence and gene compaction of the eukaryote parasite *Encephalitozoon cuniculi*. Nature. 2001; 414:450–453. [PubMed: 11719806]

Keithly JS, Langreth SG, Buttle KF, Mannella CA. Electron tomographic and ultrastructural analysis of the *Cryptosporidium parvum* relict mitochondrion its associated membranes and organelles. J. Eukaryot. Microbiol. 2005; 52:132–140. [PubMed: 15817118]

Keohane, EM.; Weiss, LM. The structure, function, and composition of the microsporidian polar tube. In: Wittner, M., editor. The Microsporidia and Microsporidiosis. ASM Press; Washington, DC: 1999. p. 196-224.

Keohane E, Takvorian PM, Cali A, Tanowitz HB, Wittner M, Weiss LM. The identification and characterization of a polar tube reactive monoclonal antibody. J. Eukaryot. Microbiol. 1994; 41:48S. [PubMed: 7804249]

Keohane EM, Takvorian PM, Cali A, Tanowitz HB, Wittner M, Weiss LM. Identification of a microsporidian polar tube protein reactive monoclonal antibody. J. Eukaryot. Microbiol. 1996; 43:26–31. [PubMed: 8563706]

Konrad C, Spycher C, Hehl AB. Selective condensation drives partitioning and sequential secretion of cyst wall proteins in differentiating *Giardia lamblia*. PLoS Pathog. 2010; 6:e1000835. [PubMed: 20386711]

Ladinsky MS, Mastronarde DN, McIntosh JR, Howell KE. Golgi structure in three dimensions: functional insights from the normal rat kidney cell. J. Cell Biol. 1999; 144:1135–1149. [PubMed: 10087259]

Ladinsky MS, Kremer JR, Furcinitti PS, McIntosh JR, Howell KE. HVEM tomography of the *trans*-Golgi network: structural insights and identification of a lace-like vesicle coat. J. Cell Biol. 1994; 127:29–38. [PubMed: 7929568]

Ladinsky MS, Wu CC, McIntosh S, McIntosh JR, Howell KE. Structure of Golgi and distribution of reporter molecules at 20C reveals the complexity of the exit compartments. Mol. Biol. Cell. 2002; 13:2810–2825. [PubMed: 12181348]

Lowman PM, Takvorian PM, Cali A. The effects of elevated temperatures and various time-temperature combinations on the development of *Brachiola (Nosema) algerae* n. comb. in mammalian cell culture. J. Eukaryot. Microbiol. 2000; 47:221–234. [PubMed: 10847338]

Lujan HD, Marotta A, Mowatt MR, Sciaky N, Lippincottschwartz J, Nash TE. Developmental induction of Golgi structure and function in the primitive eukaryote *Giardia Lamblia*. J. Biol. Chem. 1995; 270:4612–4618. [PubMed: 7876232]

McIntosh JR, Nicastro D, Mastronarde DN. New views of cells in 3D: an introduction to electron tomography. Trends Cell Biol. 2005; 15:43–51. [PubMed: 15653077]

Mowbrey K, Dacks JB. Evolution and diversity of the Golgi body. FEBS Lett. 2009; 583:3738–3745. [PubMed: 19837068]

Nagata T. Three-dimensional high voltage electron microscopy of thick biological specimens. Micron. 2000; 32:387–404. [PubMed: 11070359]

Novikoff AB. The endoplasmic reticulum: a cytochemist's view (a review). Proc. Natl Acad. Sci. 1976; 73:2781–2787. [PubMed: 183210]

Novikoff AB, Novikoff PM. Cytochemical contributions to differentiating GERL from the Golgi apparatus. Histochem. J. 1977; 9:525–51. [PubMed: 198392]

Novikoff AB, Goldfischer S. Nucleoside diphosphatase activity in the Golgi apparatus and its usefulness for cytological studies. Proc. Natl. Acad. Sci. USA. 1961; 47:802–10. [PubMed: 13729758]

Penczek P, Marko M, Buttle K, Frank J. Double-tilt electron tomography. Ultramicroscopy. 1995; 60:393–410. [PubMed: 8525550]

Radermacher, M. Weighted back-projection methods. In: Frank, J., editor. Electron Tomography. Plenum, New York: 1992. p. 91-115.

Rambourg A, Clermont Y, Hermo L. Three-dimensional architecture of the Golgi apparatus in the Sertoli cell of the rat. Am. J. Anat. 1979; 154:455–476. [PubMed: 86291]

Rambourg A, Jackson CL, Clermont Y. Three dimensional configuration of the secretory pathway and segregation of secretion granules in the yeast *Saccharomyces cerevisiae*. J. Cell Sci. 2001; 114:2231–2239. [PubMed: 11493663]

Scarborough-Bull A, Weidner E. Some properties of discharged *Glugea hertwigi* (Microsporida) sporoplasms. J. Protozool. 1985; 32:284–289.

Takvorian PM, Cali A. Enzyme histochemical identification of the Golgi apparatus in the microsporidian, *Glugea stephani*. J. Eukaryot. Microbiol. 1994; 41:63S–64S. [PubMed: 7804262]

Takvorian PM, Cali A. Polar tube formation and nucleoside diphosphatase activity in the microsporidian, *Glugea stephani*. J. Eukaryot. Microbiol. 1996; 43:102S–103S. [PubMed: 8822890]

Takvorian P, Weiss L, Cali A. The early events of *Brachiola algerae* (Microsporidia) infection: spore germination, sporoplasm structure, and development within host cells. Folia Parasitol. 2005; 52:118–129. [PubMed: 16004371]

Takvorian PM, Buttle K, Mannella CA, Weiss LM, Cali A. High voltage electron microscopy and computerized tomography: new approaches to study microsporidian spore internal organization. J. Eukaryot. Microbiol. 2006; 53:S55–S57. [PubMed: 17169067]

Tetley L, Brown SMA, McDonal V, Coombs GH. Ultrastructural analysis of sporozoite of *Cryptosporidium parvum*. Microbiology. 1998; 144:3249–3255. [PubMed: 9884216]

Touz MC, Kulakova L, Nash TE. Adaptor protein complex 1 mediates the transport of lysosomal proteins from a Golgi-like organelle to peripheral vacuoles in the primitive eukaryote. Mol. Biol. Cell. 2004; 15:3053–3060. [PubMed: 15107467]

Vavra J. Etude au microscope electronique de la morphologie et du developpement de quelques microsporidies. C. R. Acad. Sci. 1965; 261:3467–3470.

Vavra, J. Structure of the microsporidia. In: Vavra, J.; Sprague, V., editors. Biology of the Microsporidia. Vol. 1. Plenum Press; New York: 1976. p. 1-85.

Vavra, J.; Larsson, JIR. Structure of the microsporidia. In: Wittner, M.; Weiss, LM., editors. The Microsporidia and Microsporidiosis. ASM Press; Washington, DC: 1999. p. 7-84.

Vavra J, Undeen AH. *Nosema algerae* n. sp. (Cnidospora, Microsporida) a pathogen in a laboratory colony of Anopheles stephensi Liston (Diptera, Culicidae). J. Protozool. 1970; 17:240–249. [PubMed: 4915459]

Weidner E. Ultrastructural study of microsporidian invasion into cells. Z. Parasitenk. 1972; 40:227–242. [PubMed: 4346238]

Weidner E, Trager W. Adenosine triphosphate in the extracellular survival of an intracellular parasite (*Nosema michaelis*, Microsporidia). J. Cell Biol. 1973; 57:586–91. [PubMed: 4633172]

Weidner, E.; M., FA.; Dolgikh, V.; Sokolova, J. Microsporidian biochemistry and physiology. In: Wittner, M., editor. The Microsporidia and Microsporidiosis. ASM Press; Washington, DC: 1999. p. 172-195.

Xu Y, Takvorian PM, Cali A, Orr G, Weiss LM. Glycosylation of the major polar tube protein of *Encephalitozoon hellem*, a microsporidian parasite that infects humans. Infect. Immun. 2004; 72:6341–6350. [PubMed: 15501763]

Youssef N, Hammond DM. The fine structure of the developmental stages of the microsporidian *Nosema apis* (Zander). Tissue Cell. 1971; 3:283–294. [PubMed: 18631555]

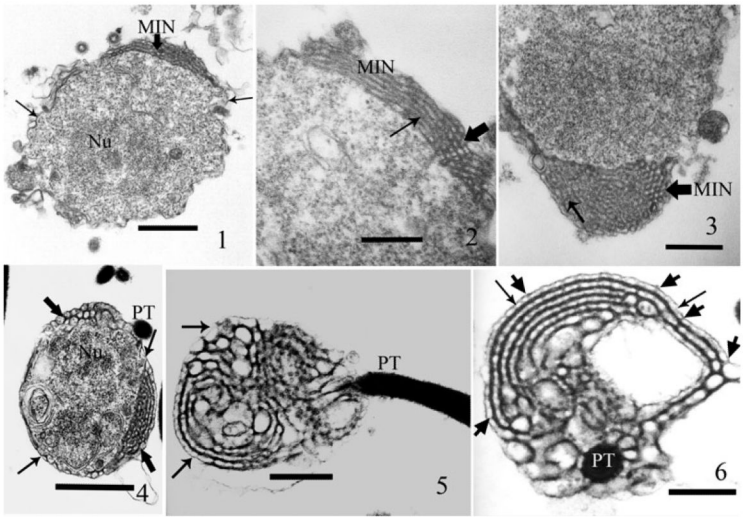

Fig. 1–6.

Germinated and extruded *Anncaliia algerae* sporoplasms 5 minutes post exposure to germination buffer, then glutaraldehyde fixed, postfixed in OsO_4, processed for thin section TEM, and stained with both uranyl acetate and lead citrate. These TEM images reveal the structure and location of the multilayered interlaced network (MIN) in the sporoplasm, and the MIN's intimate attachment to the polar tube and plasma membrane. **1**. Section through a sporoplasm. The granular cytoplasm contains a diplokaryotic nucleus (Nu) and a portion of the multilayered interlaced network (MIN) broad arrowhead. The sporoplasm is enclosed by a plasma membrane and edges of it are visible (arrows). Bar = 500 nm. **2**. A section of the sporoplasm containing a segment of the MIN that transitions from several parallel longitudinal tubules into a series of oval/round cross-sections. The broad arrowhead indicates an area of cross-sections of the MIN tubules and the thin arrow demonstrates the transition to long section of the tubules. Bar = 230 nm. **3**. A section of a sporoplasm illustrating the elaborate MIN, this angle of section shows the dense MIN within the peripheral cytoplasmic area. The broad arrowhead indicates an area of cross-sections of the MIN tubules and the thin arrow shows the transition to long section of the tubules. Bar = 300 nm. **4**. Fortuitous section through a sporoplasm enabling visualization of how, the MIN (broad arrowheads) encircles the cytoplasm immediately below the plasma membrane (thin arrows). The cytoplasm contains a diplokaryon (Nu) and the polar tube (PT) is abutted to the sporoplasm. Bar = 525 nm. **5**. A longitudinal section, through an extruded polar tube (PT), it terminates in the MIN where it attaches to the MIN tubules. The arrows indicate the less electron-dense (ED) plasma membrane encompassing the MIN. Note the variation in size and appearance of the MIN tubules and their multiple interconnections. Bar = 525 nm. **6**. Cross-section of the polar tube (PT) terminus at the region of attachment to the MIN, it illustrates its multiple connections to the MIN. Note the variable arrangement of the MIN tubules, the overlying less ED plasma membrane (arrows), and connections between both (broad arrows). Bar = 215 nm.

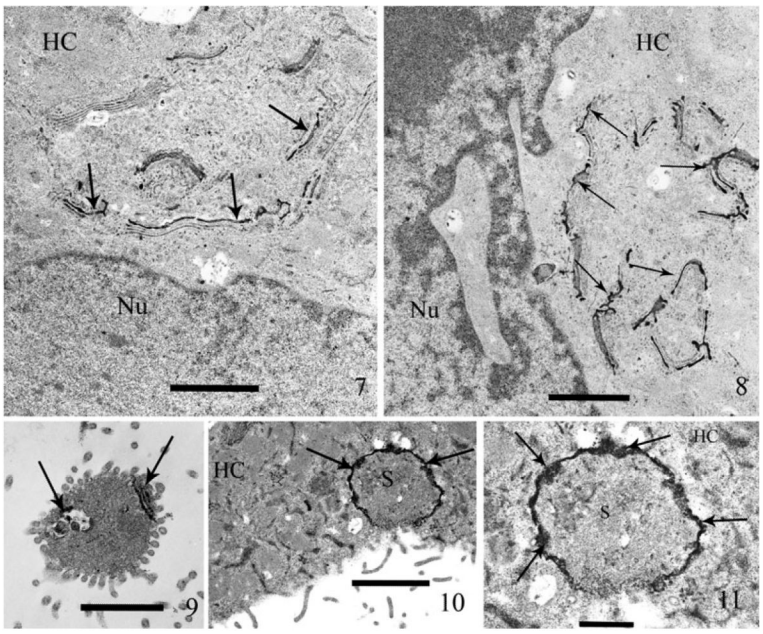

Fig. 7–11.

Thin sections of host cell cultures (RK-13) exposed to spores of *Anncaliia algerae* for one hour. Post exposure (PE) the cells were briefly immuno-fixed (glutaraldehyde and paraformaldehyde), incubated in inosine-diphosphatase (IDPase) reaction media, then processed for TEM and stained with only uranyl acetate. The deposition of electron-dense reaction product (RP) in both the host cell Golgi cisternae and the sporoplasm MIN by this enzyme histochemical reaction, demonstrates the presence of enzymes indicative of *cis*-Golgi in both the host cell and MIN. **7**. A mammalian host cell containing dense RP in the *cis*-Golgi cisternae (arrows) and some light staining of associated ER. Note the lack of RP in the other cytoplasmic (HC) organelles and the nucleus (Nu). The presence of host cell *cis*-Golgi containing RP, serves as a positive control of the IDPase enzyme histochemical labeling. The transverse section of the cisternae, appear as a series of parallel structures. Bar = 1.4 μm. **8**. Higher magnification of a second host cell, containing several areas of IDPase labeled Golgi. This section further illustrates the specificity of the histochemical reaction labeling the *cis*-Golgi (arrows). Note the host cytoplasm (HC) and nucleus (Nu) are free of RP. Bar = 1.2 μm. **9**. An extruded extracellular sporoplasm containing RP in the MIN (arrows), this label demonstrates the presence of IDPase activity in the MIN, indicating *cis*-Golgi properties. Note the rest of the sporoplasm cytoplasm is free of RP. Bar = 1.4 μm. **10**. Sporoplasm (S), intracellularly located in a host cell cytoplasm (HC). Note the presence of dense IDPase label (arrows) in the peripheral region of the sporoplasm. Bar = 1.7 μm. **11**. Higher magnification of Fig. 10. The host cell cytoplasm (HC) contains an IDPase labeled Sporoplasm (S) illustrating the presence of the electron-dense RP. The thick coat of RP (arrows) encompasses the entire periphery of the sporoplasm at the interface with the host cell. Bar = 600 nm.

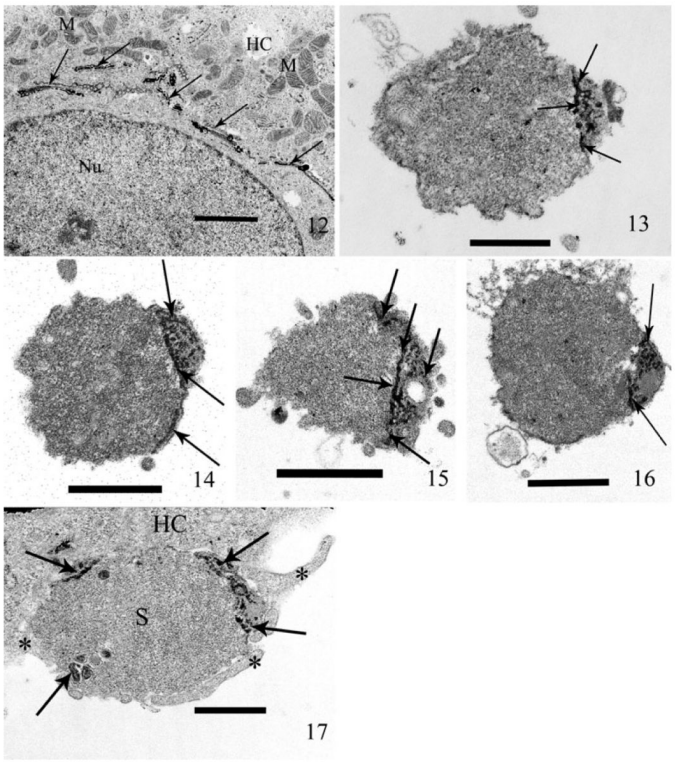

Fig. 12–17.

Thin sections of host cell cultures (RK-13) exposed to spores of *Anncaliia algerae* for 1 h. Post exposure (PE), the cells were briefly immuno-fixed (glutaraldehyde and paraformaldehyde), incubated in thiamine pyrophosphatase (TPPase) reaction media, then processed for TEM and stained with only uranyl acetate. The deposition of electron-dense RP in the host cell *trans*-Golgi cisternae provides a positive control for the TPPase histochemical label. The labeling of the sporoplasm by this enzyme histochemical reaction, demonstrates the presence of enzyme indicative of the *trans*-Golgi in the MIN. **12**. A mammalian host cell containing dense RP in the *trans*-Golgi cisternae (arrows). The presence of host cell *trans*-Golgi containing RP, serves as a positive control of the TPPase enzyme histochemical labeling. The transverse section of the cisternae, appear as a series of parallel structures, whereas those cut consistent with the cisternae provide a honey-comb like structure. Note the lack of RP in the host cell cytoplasm (HC), mitochondria (M), and the nucleus (Nu). Bar = 1.7 μm. **13**. Germinated extracellular sporoplasm labeled with TPPase. The RP is deposited in a dense cluster in the peripheral region of the cell (arrows). Bar = 500 nm. **14**. Extracellular sporoplasm labeled with TPPase. The RP appears as a dense cap in the cell and continues along the periphery (arrows) demonstrating the subplasma membrane location of the MIN. Bar = 800 nm. **15**. Extracellular sporoplasm labeled with TPPase. The RP appears as a dense ring traversing the cell and in several isolated clusters (arrows) are also present. Bar = 800 nm. **16**. Extracellular sporoplasm labeled with TPPase. The label is distributed in a ring and several short areas of dense RP (arrows) indicate the deposition in several tubular structures of the MIN. Note the presence of TPPase RP is present in the areas demonstrated to be MIN. Bar = 800 nm. **17**. The sporoplasm (S) is in the process of being phagocytized into the host cell (HC) by pseudopods (*). This may represent a mechanism for internalization of the sporoplasm leading to productive infection. Note the presence of the dense TPPase RP in several areas (arrows) and especially at the periphery of the sporoplasm where it interfaces with the host cytoplasm. This demonstrates the presence

and subplasma membrane distribution of the *trans*-Golgi enzyme TPPase in the sporoplasm MIN. Bar = 600 nm.

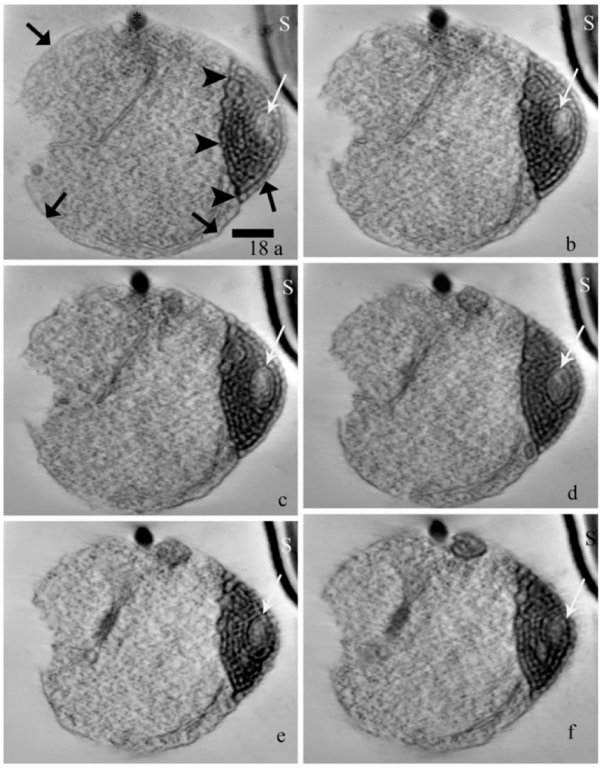

Fig. 18.

(**a–f**) Six axial slices (each representing a thickness of 4-nm) from the tomographic reconstruction of a 400-nm-thick section of a sporoplasm containing a prominent MIN. The slices were selected sequentially at intervals of approximately 20 (80-nm) to provide a representative sampling of the information in the reconstructed volume. (The entire volume is displayed as a “walk–through” Movie S1.) Note the subtle changes in the appearance of the MIN (white arrows), the sporoplasm plasma membrane (broad arrows) and the edge of the MIN (arrowheads) through the volume, the relationship between the MIN and overlying plasma membrane is visible in images a and c. The distance between the sporoplasm and an adjacent spore (S) at the upper right hand corner of the field increases at increasing depth in the tomogram. Images a–f represent slices 2, 22, 40, 64, 83, and 95, respectively. Bar = 300 nm.

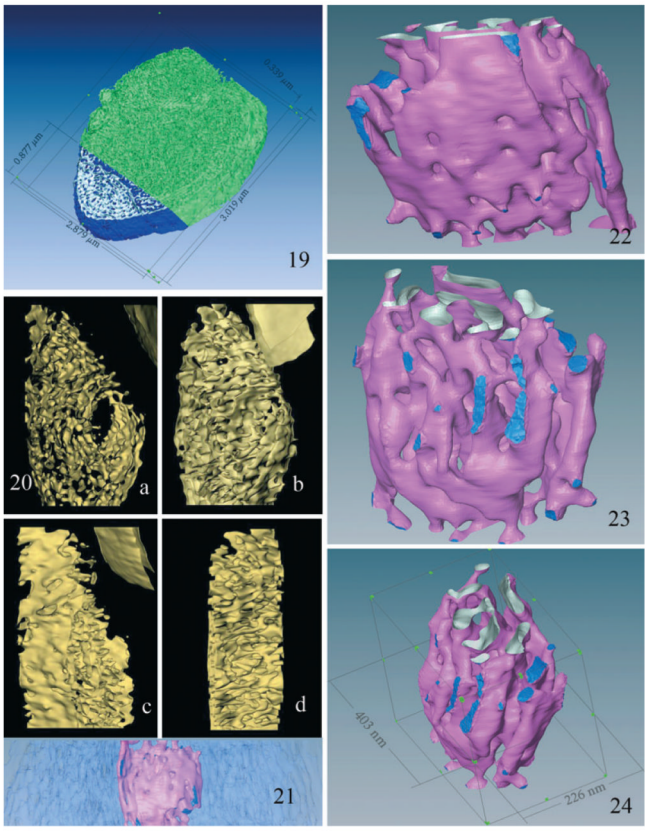

Fig. 19–24.

Three- dimensional models of the MIN-Golgi generated from HVEM images. **19**. Surface model of the central 85% of the sporoplasm tomogram. The MIN dimensions suggest that it accounts for approximately 20% of the sporoplasm volume. The external surfaces of the MIN are colored blue, the internal surfaces silver, and the rest of the volume green. **20**. **(a–d)** Four rotational views of a 3D model of the tomogram, with density thresholds set to optimally visualize local MIN surfaces. The MIN appears as a complex series of interconnected flattened sacs and tubules, not apparent in individual sections, similar to the appearance of Golgi cisternae. Note the absence of vesicles (COP-I, II) and clathrin coated buds in the models. (**a**) This view depicts the extensive series of interconnected flattened sacs and varicose tubules, which comprise the MIN. The centrally located oval "opening" represents the low-density structure indicated by the white arrow in Fig. 18a–f. The small portion of the spore edge in the upper right hand corner of the image serves as a point of orientation. (b) This view shows the transition/attachment of several of the tubules into flattened sacs and the presence of sheet-like structures. Note the change in orientation of the MIN compared to the spore edge. (**c**) This view [rotated approximately 90° from (b)] depicts the fenestrated flattened sheet-like structural aspects of the MIN. It also illustrates the edge-views of the openings of these saccuoles and tubules. (**d**) This view depicts short portions of fenestrated flattened sheets attached by numerous saccular and tubular structures. Several of the anastomosing tubules appear to be blind finger-like ends, whereas others are part of complex multiple connections. **21–24**. These are surface renderings of the central lower density subregion of the MIN in the tomogram. The flattened appearance of some of the structures is very reminiscent of the "flattened sacs" of Golgi cisternae. **21**. An edge view of the full 400-nm-thick slab of the sporoplasm, with the main area of the MIN in light blue and the lower density subregion in pink. **22**. A surface model of the low-density MIN

subregion enlarged and isolated from its surrounding high density area. The pink surfaces illustrate flattened sheets of membrane and tubules of various sizes. The upper region shows the cut tubules, with inner surfaces of the membrane sheets illustrated in silver. The lower portion of the model illustrates the branched tubular networks and the presence of some interconnections. The dark blue areas represent contacts or interfaces of the subregion with the higher density surrounding MIN region. **23**. This view of the MIN is rotated and tilted with respect to Fig. 22. It depicts the branched varicose tubules, which taper and appear to constrict in some areas, whereas other tubules intersect and form flattened dilations that increase in size. **24**. Another view of the surface model in Fig. 22, 23, providing the dimensions along each axis.